Particle Accelerators
1984 Vol. 16 pp. 39–62
0031-2460/84/1602–0039$25.00/0

COMPUTATION OF CLOSED ORBITS AND BASIC FOCUSING PROPERTIES FOR SECTOR-FOCUSED CYCLOTRONS AND THE DESIGN OF "CYCLOPS"†

M. M. GORDON

National Superconducting Cyclotron Laboratory
Michigan State University
East Lansing, MI 48824

(*Received November 7, 1983*)

The program Cyclops, like the Equilibrium Orbit Code before it, calculates with optimum efficiency all the important properties of the closed orbits and of the linear radial and vertical oscillations about these orbits. Such orbits include both normal equilibrium orbits and those displaced by field perturbations, as well as unstable fixed-point orbits associated with certain nonlinear resonances. Given the median-plane magnetic field in polar coordinates, the program uses direct numerical integration of the canonical equations of motion (together with special iteration and extrapolation procedures for obtaining the correct initial conditions) to calculate these orbit properties as a function of the ion energy over the range available in the given field. At each energy, the output provides values of the focusing frequencies, eigenellipse parameters, and form factors for the linear oscillations, as well as data on the frequency error and phase slip. A reasonably detailed discussion is presented of the theoretical basis for these calculations, along with some applicatons of the results to the design and analysis of sector-focused cyclotrons.

1. INTRODUCTION

Ever since its early development at Oak Ridge,[1] the Equilibrium Orbit Code has been one of the most-useful computer programs available to those engaged in the design and analysis of sector-focused cyclotrons. Given the median-plane field $B(r, \theta)$ in polar coordinates, this program computes at each energy all the important properties of the equilibrium orbit (*EO*) and of the linear radial and vertical oscillations about this orbit. These include, of course, the orbit period τ and the focusing frequencies ν_r and ν_z.

The *EO* Code is based on direct numerical integration of the canonical equations of motion, and the key element of this program is the efficient iteration scheme by which it determines the *EO* coordinates r and p_r as a function of θ. Such a scheme is practically essential, since for sector-focused cyclotrons with isochronous fields, the shape of the *EO* generally changes with energy and the q/m of the ion, as well as the magnet excitation.

As was discovered somewhat later, the *EO* Code can also be used to calculate any other closed orbit in the median plane of the given field.[2] Such orbits include, for

† Work supported by the National Science Foundation under Grant No. Phy 78-22696.

example, the unstable fixed-point orbits associated with $\nu_r = N/3$ or $N/4$ nonlinear resonance. In such cases, the program produces data showing the variation of the stability limits with energy, and thereby assists in the construction of radial phase-space diagrams. Recent examples of these applications are shown in Figs. 1 and 2.

Moreover, when imperfections are added to the median-plane field, the same iteration scheme enables the program to locate the displaced *EO*'s or other fixed-point orbits. At the same time, the program provides values of ν_r and ν_z for the displaced orbits, and this information helps in evaluating possible resonance effects produced by the given field imperfections. See, for example, Fig. 2.

One should, of course, keep in mind that the results of analytical treatments of most (but not all) of these phenomena have long been available through the work of Smith and Garren,[3] Parzen,[4] and especially Hagedoorn and Verster.[5] These analytical results are most useful in revealing how various orbit properties depend on specific parameters of the magnetic field. However, when highly accurate results are required on a routine basis, then the *EO* Code becomes practically indispensible.

The first Fortran version of this program was completed in 1964 and named Cyclops, short for Cyclotron Closed Orbit Program.[6] Not long thereafter, a modified version was developed by Joho[7] in connection with the design of the large SIN Cyclotron. Later, the original Cyclops program was transferred to Vancouver, where it was adapted by Mackenzie, Kost, and coworkers for design work on the large TRIUMF cyclotron.[8] In particular, this group developed an extended version of Cyclops in order to generate the data required for a transfer-matrix program ("COMA") which very efficiently calculates large groups of accelerated orbits assuming linear, but non-adiabatic conditions.[9] More recently, the TRIUMF group has employed Cyclops in their design work on high-energy cyclotrons for possible use as "kaon factories."[10]

The main reason for writing this report now is that we are planning a new version of the Cyclops program that will incorporate all the improvements suggested by twenty years of experience here and elsewhere. Our aim, therefore, is to present a reasonably complete discussion of the theoretical basis for this program in order to make its construction and operation sufficiently clear to those who might be interested in using or writing such a program. Moreover, much of the material presented here is not generally available elsewhere.

The Cyclops program differs from the original *EO* Code mainly in the amount of information it provides on the linear oscillations. That is, the *EO* Code gives only the values of ν_r and ν_z, while Cyclops provides, in addition, such quantities as $\alpha(\theta)$ and $\beta(\theta)$, the well-known parameters characterizing the periodic transfer matrix.[11] As in synchrotron applications, these parameters can be used to find the eigenellipse properties as well as the width functions and form factors for the radial and vertical oscillations.

However, the definition and interpretation of $\alpha(\theta)$ and $\beta(\theta)$ are somewhat different from those usually found in synchrotron work. This difference results mainly from our formulation of the equations of motion, and because of this difference, we present here a somewhat more detailed discussion of the theory than would otherwise be necessary.

We should note, in particular, that because we use canonical variables, the resultant width functions automatically contain the adiabatic damping. That is, our β varies as R/p, and this form seems much more appropriate for isochronous cyclotrons where R and p increase rapidly with energy, but the ratio R/p does not.

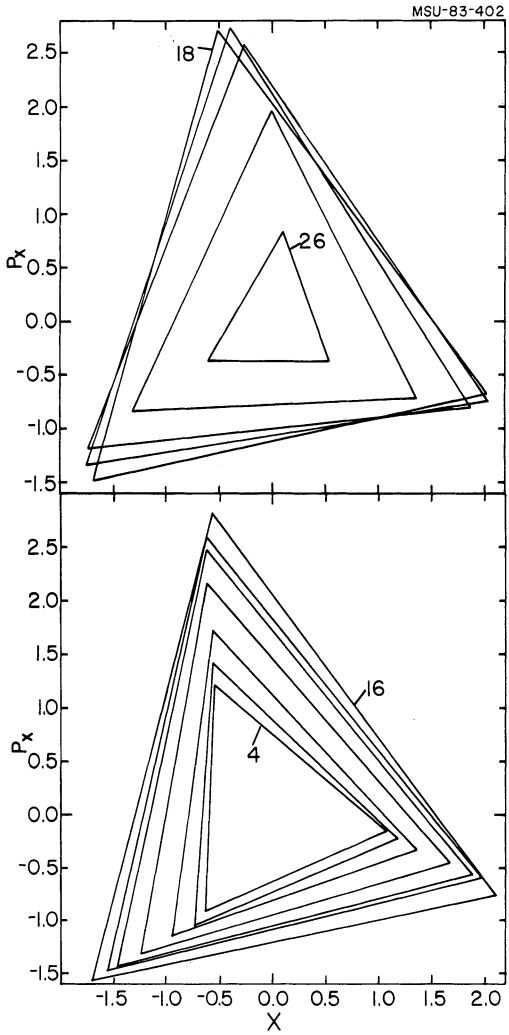

FIGURE 1 Variation of radial stability limits with energy resulting from the $\nu_r = 3/3$ nonlinear resonance in the NSCL K500 superconducting cyclotron. The magnetic field used for these calculations (and those depicted in the remaining figures) was specifically tailored for C^{4+} ions with a final energy of 30 MeV/A. At each energy, the (x, p_x) values for the three unstable fixed-point orbits are plotted here and then joined by straight lines to form the "stability triangle." These triangles are shown from 4 MeV/A out to 26 MeV/A in steps of 2 MeV/A, and as can be seen, the stable area expands out to about 18 MeV/A and then shrinks. These triangles actually start at 0.8 MeV/A and terminate at 28.8 MeV/A, where ν_r crosses $\nu_r = 1$, as shown in Fig. 4. Note that the points are plotted here not at the same θ value, but rather along the spiral curve $\theta = 30° - (4.4 \text{ deg/in.})r$, which corresponds to the linear spiral of the magnet sectors, and because of this plotting convention, the otherwise rapid rotation of the triangles with increasing radius is nearly eliminated here. We use inch units for p_x as well as x (as discussed near the end of Section 2) and in these units, accelerated orbits representing an actual beam usually have (x, p_x) points lying within a circle of radius 0.1 in. centered on the origin (EO). Note also that (x, p_x) specifies the deviation of (r, p_r) from the corresponding EO value at the same energy.

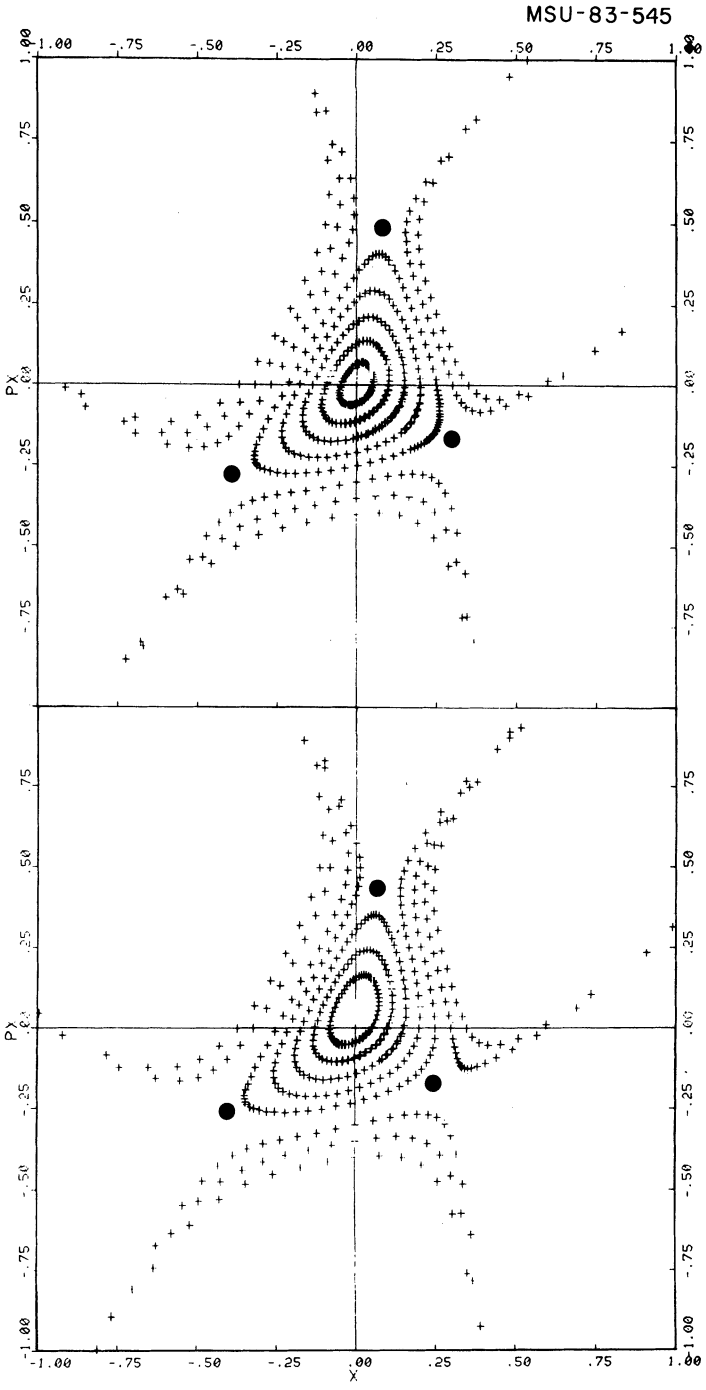

FIGURE 2 Two radial phase-space diagrams characterizing the behavior of a variety of stable and unstable orbits, all at 28 MeV/A. Each orbit is represented by a sequence of (x, p_x) points (shown as crosses) which are plotted once per turn along the same spiral curve used for Fig. 1. The data for the upper diagram were obtained with the perfect $N = 3$ field, for which $\nu_r = 1.0214$ and $\nu_z = 0.4457$ at this energy. The lower diagram was derived from the actual field and shows the changes produced by the presence of small $N' = 1$ and 2 components. In this case, $\nu_r = 1.0211$ and $\nu_z = 0.4462$ for the displaced *EO*. The three unstable fixed points are shown as solid circles and all have complex ν_z as well as complex ν_r values. For example, the fixed point closest to the *EO* in the lower diagram has $\nu_r = 1.0 + i(0.0367)$ and $\nu_z = 0.5 + i(0.0330)$. These values indicate the quantitative effects of both the $\nu_r = 3/3$ and $\nu_r = 2\nu_z$ nonlinear resonances which are evidently nearby.

2. INPUT AND UNITS

The input parameters for Cyclops are generally the same as those for the isochronous-field program described in a previous paper.[1,2] In addition to the mass m and charge q of the ion, we now require a map of the median-plane field $B(r, \theta)$ on a polar mesh having constant values of δr and $\delta\theta$, the radial and angular spacings. If the field has N sectors and no imperfections, then the map need only cover one sector, $\Delta\theta = 2\pi/N$, and the spacing $\delta\theta$ (which also defines the smallest integration step) must be an integral submultiple of this angle, i.e., $\delta\theta = 2\pi/nN$. On the other hand, if the field contains imperfections, then a complete map with $\Delta\theta = 2\pi$ is usually required. Given the field map, the program then uses interpolation formulas to obtain the necessary values of B and its derivatives, $\partial B/\partial r$ and $\partial B/\partial\theta$ at any given point.

The frequency $\nu_0 = \nu_{rf}/h$ is also part of the input, where ν_{rf} is the nominal rf frequency and h its harmonic number. Using $\omega_0 = 2\pi\nu_0$, we define an associated length unit a and field unit b as

$$a = c/\omega_0, \qquad b = m\omega_0/q. \tag{1}$$

However, use of the constants a and b is not at all mandatory.

Although the units chosen for length (inch or cm), energy (MeV), and magnetic field (kG) are quite obvious, the choice of momentum unit is not. This decision is required because all our programs use the momenta p_r and p_z as variables rather than the quantities p_r/p and p_z/p commonly used for synchrotrons. Using p_r and p_z has the advantage of making the consequences of Liouville's theorem and adiabatic invariance immediately apparent.

To be more specific, we assume that

$$\text{momentum unit} = mc/a', \tag{2}$$

where a' is some given constant independent of the energy. Thus, $p = \gamma(v/c)a'$ in this unit, or,

$$p = a'\left[\frac{E}{mc^2}\left(2 + \frac{E}{mc^2}\right)\right]^{1/2}, \tag{3}$$

where $\gamma = 1 + E/mc^2$, and E is the kinetic energy of the ion. For example, if $a' = 10^3$ (a choice preferred by Joho[7]), then p_r and p_z as well as p are effectively in millirad. If in addition, the length unit is mm, then the phase-space area (e.g., $\int dp_z\, dz$) corresponds directly to the so-called normalized emittance, i.e., $\gamma(v/c) \times$ (ordinary emittance).

In all the orbit programs currently in use at this laboratory, we take $a' = a$ so that all momenta have length units. Since $v = R\omega_0$ for an isochronous field, then $p = \gamma R$ in our units, which is often convenient. For example, in the nonrelativistic domain where $\nu_r \cong \gamma \cong 1$, then $p\nu_r/R \cong 1$ in our units, so that any orbit executing linear radial oscillations about the *EO* will be characterized by a nearly circular phase-space figure when values of p_x are plotted *vs.* x for this orbit. (See Figs. 1 and 2.) Moreover, the vector (x, p_x) in these units indicates directly both the magnitude and direction of the orbit-center displacement from the machine center. However, these advantages become less apparent for cyclotrons which are more relativistic.

3. ITERATION SCHEME

For each energy E, the program must first search for and locate the closed orbit by finding a solution of the equations of motion for which r and p_r satisfy the periodicity condition

$$r(\theta\ \theta_0) = r(\theta), \qquad p_r(\theta + \theta_0) = p_r(\theta). \tag{4}$$

The closed orbit most frequently sought is the normal *EO* in a field having N sectors and no imperfections, and in this case, $\theta_0 = 2\pi/N$ i.e., one sector. In those circumstances when the field being investigated has imperfections, or when some other closed orbit is being sought, then θ_0 will be some multiple of $2\pi/N$. For example, when $\nu_r \cong N/3$ and the orbit being sought is an unstable fixed-point orbit associated with the $N/3$ resonance, then $\theta_0 = 3(2\pi/N)$.

The values of r and p_r and generated by integrating the canonical equations of motion in the given median plane field $B(r, \theta)$, namely,

$$\frac{dr}{d\theta} = \frac{rp_r}{p_\theta}, \tag{5a}$$

$$\frac{dp_r}{d\theta} = p_\theta = q'rB(r, \theta), \tag{5b}$$

where

$$p_\theta = (p^2 - p_r^{\,2})^{1/2}, \tag{5c}$$

with p given in Eq. (3), and where $q' = qa'/mc$, with a' defined in Eq. (2). In our special units, $a' = a$, and $q' = 1/b$, with a and b defined in Eq. (1).

The complete integration interval for these differential equations (and all the others given below) is $\Delta\theta = \theta_0$, and assuming the integration starts at some given angle θ_i, the range of θ values is

$$\theta_i \leq \theta \leq \theta_f, \tag{6}$$

where $\theta_f = \theta_i + \theta_0$ is the final angle. Our problem therefore reduces to finding the pair of initial values (r_i, p_{ri}) at $\theta = \theta_i$ which lead to the same final values when the integration is completed, i.e., which satisfy

$$r(\theta_i + \theta_0) = r_i, \qquad p_r(\theta_i + \theta_0) = p_{ri}, \tag{7}$$

in accordance with Eq. (4) above. These all-important initial values can be efficiently determined by a straightforward iteration process which is an extension of the familiar Newton method.

We first introduce the differential equations for the linear radial oscillations since the solution of these equations plays an important role in the iteration process as well as the final determination of the basic focusing properties. Since Eqs. (5) apply quite generally to any (non-accelerated) orbit in the median plane, they can be used to obtain the linear oscillation equations simply by allowing

$$r \to r + x, \qquad p_r \to p_r + p_x, \tag{8}$$

and then expanding the equations to first order in x and p_x. When this is done, we find

$$\frac{dx}{d\theta} = \frac{p_r}{p_\theta} x + \frac{rp^2}{p_\theta{}^3} p_x, \tag{9a}$$

$$\frac{dp_x}{d\theta} = -\frac{p_r}{p_\theta} p_x - q'\left[B + r\frac{\partial B}{\partial r}\right] x, \tag{9b}$$

where r and p_r have the same values at each θ as those used on the right side of Eqs. (5) during the integration.

In order to generate the basic transfer matrix, we need two independent solutions of these equations, and these are denoted as (x_1, p_{x_1}) and (x_2, p_{x_2}). For initial conditions, it proves most convenient to choose

$$\left.\begin{aligned} x_1(\theta_i) &= 1, \qquad p_{x_1}(\theta_i) = 0, \\ x_2(\theta_i) &= 0, \qquad p_{x_2}(\theta_i) = 1, \end{aligned}\right\} \tag{10}$$

and in this case, the transfer matrix from θ_i to a given θ is defined by

$$\mathbf{X}(\theta, \theta_i) = \begin{pmatrix} x_1 & x_2 \\ p_{x_1} & p_{x_2} \end{pmatrix}_\theta \tag{11}$$

so that $\mathbf{X}(\theta_i, \theta_i) = \mathbf{I}$, the unit matrix. Hence, the general solution of (9) can be written in matrix form as

$$\begin{pmatrix} x \\ p_x \end{pmatrix}_\theta = \mathbf{X}(\theta, \theta_i) \begin{pmatrix} x \\ p_x \end{pmatrix}_i. \tag{12}$$

Note that the Wronskian relation (or Liouville's theorem) leads to the value for the determinant

$$\|\mathbf{X}(\theta, \theta_i)\| = x_1(\theta) p_{x_2}(\theta) - x_2(\theta) p_{x_1}(\theta) \equiv 1, \tag{13}$$

its initial value. Also note that because of the choice (10), the elements of $\mathbf{X}$ automatically have the correct units.

Each cycle of the iteration process starts with a trial value for the pair (r_i, p_{ri}). These initial conditions, along with those in Eq. (10), are then used to carry out the integration of the six differential equations noted above, namely, Eqs. (5) for r and p_r, the coordinates of the trial orbit, and two sets of Eqs. (9) for the elements of the matrix $\mathbf{X}(\theta, \theta_i)$ of Eq. (11), which is associated with this trial orbit. All six differential equations are integrated simultaneously, since this proves most efficient for standard integration routines.

When the integrations are completed at $\theta = \theta_f$, the errors in the trial values of (r_i, p_{ri}) are calculated from

$$\epsilon_1 = r(\theta_f) - r_i, \qquad \epsilon_2 = p_r(\theta_f) - p_{ri}, \tag{14}$$

where $\theta_f = \theta_i + \theta_0$. If these errors are not both zero, as required by the periodicity condition, we proceed to calculate improved trial values. To do so, we assume the true

closed orbit differs from the trial orbit only in first order, and using Eq. (12), we can therefore write

$$\begin{pmatrix} r_c \\ p_{rc} \end{pmatrix}_\theta = \begin{pmatrix} r \\ p_r \end{pmatrix}_\theta + \mathbf{X}(\theta, \theta_i) \begin{pmatrix} \delta r_i \\ \delta p_{ri} \end{pmatrix}, \tag{15a}$$

so that $r_c(\theta_i) = r_i + \delta r_i$, and $p_{rc}(\theta_i) = p_{ri} + \delta p_{ri}$. Thus, (r_c, p_{rc}) and (r, p_r) are, respectively, the coordinates of the closed orbit and the trial orbit (already computed), and δr_i and δp_{ri} are the corrections being sought.

Applying this equation at $\theta = \theta_i$ and $\theta = \theta_f$, and taking the difference, we then obtain

$$0 = \begin{pmatrix} \epsilon_1 \\ \epsilon_2 \end{pmatrix} + [\mathbf{X}(\theta_f, \theta_i) - \mathbf{I}] \begin{pmatrix} \delta r_i \\ \delta p_{ri} \end{pmatrix} \tag{15b}$$

which then yields the corrections

$$\delta r_i = \frac{(X_{22} - 1)\epsilon_1 - X_{12}\epsilon_2}{X_{11} + X_{22} - 2}, \tag{16a}$$

$$\delta p_{ri} = \frac{(X_{11} - 1)\epsilon_2 - X_{21}\epsilon_1}{X_{11} + X_{22} - 2}, \tag{16b}$$

where here $X_{jk} = X_{jk}(\theta_f, \theta_i)$. Thus we see that the change

$$r_i \to r_i + \delta r_i, \qquad p_{ri} \to p_{ri} + \delta p_{ri}, \tag{17}$$

will provide improved values for the initial conditions, and these values are then used to repeat the entire process in the next cycle.

Before proceeding, however, we first calculate the amplitude of the error defined by

$$\epsilon = \frac{1}{r_i}\left[(\delta r_i)^2 + \left(\frac{a\,\delta p_{ri}}{a'\gamma^2}\right)^2\right]^{1/2}, \tag{18}$$

where the factor $a/a'\gamma^2$ has been inserted to make the two terms commensurate. This ϵ is approximately equal to the maximum value of x/R for the oscillation produced by the error, so that the smallness of ϵ provides a test of whether the closed orbit has been located with sufficient accuracy. Hence we test whether

$$\epsilon < \epsilon_0 \tag{19}$$

where ϵ_0 is a pre-assigned error limit discussed later. If ϵ fails the test, the program proceeds to the next cycle of the iteration process.

This process converges quite rapidly once a threshold value of ϵ has been reached. That is, the corrections in Eq. (16) are exact to first order, so that if ϵ is small, the error in the improved value will be of order ϵ^2. Thus, the sequence of errors on successive iterations will be of order ϵ, ϵ^2, ϵ^4, ϵ^8, etc.

4. STARTING VALUES

The total number of iterations and, hence, the time required for the process to converge depends entirely on the quality of the starting values for r_i and p_{ri}. When the calculations concern the *EO* itself, and when no other data are available for guidance, we generally use the approximate values

$$r_i = (v/c)a, \qquad p_{ri} = 0, \tag{20}$$

which correspond to a nearly isochronous field with $\omega_0 = c/a$. Alternatively, r_i could be obtained by solving the equation $p = q' r_i B_0(r_i)$, where $B_0(r)$ is the average field. Either choice will usually work, and will actually work very well when the *EO* is nearly circular, i.e., when the flutter is small or N is large.

Normally, the program is run at a long sequence of energy values and, in this case, a considerable saving of time can be achieved by using an extrapolation method for obtaining succeeding starting values. If $r_i(E)$ and $p_{ri}(E)$ are the final "exact" values found for these quantities, then the extrapolation is based on the scaled variables

$$\xi_1 = \frac{r_i(E)}{(av/c)}, \qquad \xi_2 = \frac{p_{ri}(E)}{p}, \tag{21}$$

since these quantities vary more slowly with E, especially near $r = 0$. Thus, when no other data are given, the program uses Eq. (20) for the first E value, then a one-point extrapolation formula with the variables ξ_1 and ξ_2 for the second E value, and then a two-point formula with these variables for the third E value. From then on, it uses a three-point formula with data from the three previous E values.

This extrapolation routine works very well once it reaches the three-point stage. With this in mind, the program should be designed with a "fast mode" option wherein, after the first three energy values are completed, it then skips the test Eq. (19) and proceeds instead to the final integration described in the next section. This fast mode is most useful when a large number of runs are required, as in the calculation of isochronous fields and trim coil currents.[12] In such cases, it is often worth trading some accuracy for increased speed. Moreover, the accuracy can always be monitored since the program prints out the value of $\log \epsilon$ using the very last value of ϵ.

Although the foregoing procedure is designed primarily for normal *EO* calculations, it will also work quite well when calculating the properties of displaced *EO*'s resulting from field imperfections. A slight modification is required, however, when investigating other closed orbits such as, e.g., the unstable fixed-point orbits associated with nonlinear resonances.

This modification simply involves replacing Eq. (20) by specific starting values for r_i and p_{ri} at the first energy. These values can be obtained, e.g., by constructing (with the aid of a straightforward orbit-computation program) phase-space plots of p_r vs r at the given E, and then examining these plots visually to determine an approximate value for the pair r_i and p_{ri}. If Cyclops uses these input data successfully to locate the desired fixed-point orbit at the first E value, then, by using the extrapolation technique described above, it will generally have no difficulty in finding these orbits at the succeeding E values.

As often happens, there may be more than one closed orbit with the given periodicity θ_0, and in such cases, the program will usually select the one with (r_i, p_{ri}) closest to the given (or computed) starting values. Thus, when tracking a particular fixed-point orbit

at a sequence of energies, one sometimes finds on reaching a certain E value, that the program locates the *EO* instead. This occurrence usually indicates that the fixed-point orbit and the *EO* have merged, or are about to merge. Such is the case, for example, when ν_r passes through $N/3$.

5. FINAL INTEGRATION

The iteration process described above for determining (r_i, p_{ri}) has a well-defined convergence rate, and as a result, the test (19) on ϵ can be established so that the "correct" values of r_i and p_{ri} can be inferred quite well without requiring an additional iteration cycle for confirmation. For example, if it is desired that the closed orbit be determined with an accuracy such that the test (19) is satisfied for $\epsilon_0 = 10^{-8}$, say, then this test should actually be made with $\epsilon_0 = 10^{-4}$ since, as we have seen, the improved (r_i, p_{ri}) derived from Eq. (16) will then be in error by only the square of this quantity. The program will still make another integration of the differential equations so that the final value of ϵ can be checked, but before this integration is performed, certain changes need to be made.

On the final integration, the program calculates all the data required to determine completely the properties of the closed orbit and of the linear radial and vertical oscillations. The two differential Eqs. (5) are integrated with the now "correct" (r_i, p_{ri}) so that the resulting $r(\theta)$ and $p_r(\theta)$ give the coordinates of the actual closed orbit. Two sets of the differential Eqs. (9) are also integrated as before with initial conditions (10) so as to generate the transfer matrix $\mathbf{X}$ in Eq. (11). But since the r and p_r are now the correct closed-orbit coordinates, the resultant $\mathbf{X}$ will accurately characterize the linear radial oscillations about this orbit. To these six differential equations, which are the same as those used in the iteration process, we now add at least six more, all of which are integrated simultaneously to optimize efficiency.

When expressed in canonical form, the equations for the linear vertical oscillations become

$$\frac{dz}{d\theta} = \frac{r}{p_\theta} p_z, \tag{22a}$$

$$\frac{dp_z}{d\theta} = q'\left[r \frac{\partial B}{\partial r} - \frac{p_r}{p_\theta} \frac{\partial B}{\partial \theta} \right] z, \tag{22b}$$

where r, p_r, and p_θ have the same values as those used in Eqs. (5) and (9). Here again, two solutions of these equations are required in order to generate the basic transfer matrix, and by analogy to Eq. (10), these are denoted as (z_1, p_{z1}) and (z_2, p_{z2}), and have the initial conditions

$$\left.\begin{aligned} z_1(\theta_i) &= 1, \qquad p_{z_1}(\theta_i) = 0, \\ z_2(\theta_i) &= 0, \qquad p_{z_2}(\theta_i) = 1, \end{aligned}\right\}, \tag{23}$$

so that the transfer matrix $\mathbf{Z}(\theta, \theta_i)$ for the vertical oscillations is given by

$$\mathbf{Z}(\theta, \theta_i) = \begin{pmatrix} z_1 & z_2 \\ p_{z_1} & p_{z_2} \end{pmatrix}_\theta, \tag{24}$$

by analogy to Eq. (11). This $\mathbf{Z}(\theta, \theta_i)$ provides complete information about the linear vertical oscillations, just as $\mathbf{X}(\theta, \theta_i)$ does for the radial oscillations.

In addition to the ten listed above, we need two or more differential equations to provide necessary information about the time coordinate and the geometry of the closed orbit. The differential equation for the time t (which is also canonical) is written as

$$\frac{d}{d\theta}(\omega_0 t) = m'\gamma \frac{r}{p_\theta}, \tag{25}$$

where $\gamma = 1 + E/mc^2$, as usual, and $m' = a'/a$ in the units of Eq. (2). This equation is integrated with the initial condition $t = 0$ at $\theta = \theta_i$, and we therefore have at $\theta_f = \theta_i + \theta_0$,

$$\omega_0 t(\theta_f) = \frac{\theta_0}{2\pi}\omega_0\tau = \theta_0\frac{\omega_0}{\omega}, \tag{26}$$

where $\omega = 2\pi/\tau$, and τ is the orbit period (for the *EO*, at least). This result provides the frequency error Ω defined by

$$\Omega(E) = \frac{\omega_0}{\omega} - 1, \tag{27}$$

and this function plays an important role in the phase-energy relation discussed in Section 10 below.

Another differential equation is usually included in order to determine the average radius R_0 defined by

$$R_0 = \frac{1}{\theta_0}\int r(\theta)\, d\theta, \tag{28}$$

where the integration extends from θ_i to $\theta_i + \theta_0$. Although this R_0 is part of our standard output, others prefer instead the average radius based on the arc length

$$R = \frac{v\tau}{2\pi} = \frac{\omega_0}{\omega}\frac{v}{c}a, \tag{29}$$

which can be obtained directly from Eq. (26). Note that $R \geq R_0$.

Since it requires very little extra effort, the program should be equipped to generate the data needed to calculate the changes in t resulting from a linear displacement (x, p_x) from the closed orbit, particularly the *EO*. The necessary differential equation can be obtained simply by expanding Eq. (25).

First we define a time-displacement variable χ such that if

$$r \to r + x, \qquad \text{and} \qquad p_r \to p_r + p_x, \tag{30a}$$

then

$$\omega_0 t \to \omega_0 t + \chi. \tag{30b}$$

Next we expand Eq. (25) to first order and thereby obtain

$$\frac{d\chi}{d\theta} = m'\gamma\left[\frac{x}{p_\theta} + \frac{rp_r}{p_\theta^3}p_x\right], \tag{31}$$

which is the differential equation being sought.

Here again two solutions are required in general, and we denote them as χ_j with $j = 1$ or 2, corresponding to the two basic solutions (x_j, p_{xj}) in Eq. (10) which are being generated simultaneously during the final integration. For initial conditions, we take $\chi_j = 0$ at $\theta = \theta_i$.

An important application of the functions $\chi_j(\theta)$ is in the construction of a transfer-matrix program that includes acceleration effects through the use of delta-function gaps. That is, given x, p_x, and χ at θ_i for some displaced orbit, then the value of χ at any other θ is

$$\chi(\theta) = \chi(\theta_i) + \chi_1(\theta)x(\theta_i) + \chi_2(\theta)p_x(\theta_i), \tag{32}$$

while the value of x and p_x at θ are still given by Eq. (12) in terms of the matrix $\mathbf{X}(\theta, \theta_i)$. The TRIUMF program "COMA" mentioned before uses such a formalism.[9]

It should be noted here that since we are considering only linear motion, the dependence of t on z and p_z can be neglected. It should also be noted that an alternative method is available for treating the dependence of t on x and p_x without the use of χ_j.[13]

6. CALCULATION OF ν_r AND ν_z

The program can provide either a short (standard) output or a long output, which differ mainly in the amount of information given on the linear oscillations. In the short output, only the values of ν_r and ν_z are printed out.

Since there is a complete analogy between the equations for the radial oscillations and those for the vertical oscillations, we simplify the discussion by letting y stand for either x or z. Thus, e.g., the matrix $\mathbf{Y}$ stands for $\mathbf{X}$ or $\mathbf{Z}$, while ν_y stands for either ν_r or ν_z.

At the end of the final integration, the elements of $\mathbf{Y}(\theta_f, \theta_i)$ are all known, and since $\theta_f = \theta_i + \theta_0$, we recognize that $\mathbf{Y}(\theta_f, \theta_i)$ is the transfer matrix for one complete period starting at θ_i. Hence, in accordance with Floquet's theorem, the eigenvalues of this matrix are

$$\lambda = \exp(\pm i\sigma), \tag{33a}$$

where

$$\sigma = \nu_y\theta_0, \tag{33b}$$

and

$$\cos\sigma = \frac{1}{2}[Y_{11}(\theta_f, \theta_i) + Y_{22}(\theta_f, \theta_i)]. \tag{33c}$$

Thus, if $|\cos\sigma| \leq 1$, then σ is real and the motion is stable, but if $|\cos\sigma| > 1$, then σ is complex and the motion is generally unstable.

In keeping with general practice, we write the matrix $\mathbf{Y}(\theta_f, \theta_i)$ in the standard form

$$\mathbf{Y}(\theta_f, \theta_i) = \mathbf{I} \cos \sigma + \mathbf{J}(\theta_i) \sin \sigma, \tag{34a}$$

where $\mathbf{I}$ is again the unit matrix, and

$$\mathbf{J}(\theta_i) = \begin{pmatrix} \alpha_i & \beta_i \\ -\gamma_i & -\alpha_i \end{pmatrix}, \tag{34b}$$

which defines the parameters α_i, β_i, and γ_i. These quantities are then related to the known matrix elements by

$$\alpha_i \sin \sigma = \frac{1}{2}[Y_{11}(\theta_f, \theta_i) - Y_{22}(\theta_f, \theta_i)], \tag{35a}$$

$$\beta_i \sin \sigma = Y_{12}(\theta_f, \theta_i), \tag{35b}$$

$$\gamma_i \sin \sigma = -Y_{21}(\theta_f, \theta_i), \tag{35c}$$

and since, moreover, $\| \mathbf{Y} \| = 1$ from Eq. (13), we also have

$$\beta_i \gamma_i - \alpha_i^2 = 1, \tag{35d}$$

which serves to determine γ_i from α_i and β_i. Thus, the elements of $\mathbf{Y}(\theta_f, \theta_i)$ are reduced to the three independent parameters α_i, β_i, and σ.

When σ is real, we again follow convention by assuming $\beta_i > 0$, and we therefore find from Eq. (35b) that the sign of $\sin \sigma$ matches that of $Y_{12}(\theta_f, \theta_i)$. As a result, Eqs. (33) and (35) determine $\sin \sigma$ as well as $\cos \sigma$, and the value of $\sigma = \nu_y \theta_0$ can therefore be calculated modulo 2π.

Assuming $0 \leq \nu_y \theta_0 < 2\pi$, the *EO* Code uses this procedure to calculate the values of ν_r and ν_z when these quantities are real. On the other hand, when $|\cos \sigma| > 1$, so that the motion is unstable, the program uses $|\cos \sigma|$ to find the imaginary part of ν_r or ν_z, which is then printed out with a special indicator.

For the normal *EO*, the values of ν_r and ν_z always lie below the $N/2$ stop-band, so that as long as $\theta_0 = 2\pi/N$, only σ values below π will occur. Moreover, complex values are encountered only when ν_z^2 drops below zero, as sometimes occurs when the relativistic defocusing predominates over the sector focusing. In these cases, the foregoing procedure yields the correct values of ν_r and ν_z.

However, this is generally not true when the closed orbit is a displaced *EO* or an unstable fixed point. Consider, e.g., the data shown in Fig. 2 which results from an $N = 3$ magnet geometry with small $N' = 1$ and 2 imperfections. Because of these perturbations, the calculations must be carried out with $\theta_0 = 2\pi$ rather than $2\pi/3$, and in this case, the program prints out $\nu_r' = 0.0211$ instead of the correct value $\nu_r = 1.0211$ which can be inferred from the value ($\nu_r = 1.0214$) obtained when the imperfections are absent.

Clearly, additional information is needed in such cases to remove the uncertainty. To obtain this information, we assume that in general

$$\sigma = n\pi + \sigma', \tag{36}$$

where n is an integer, and where $0 \leq \sigma' \leq \pi$ if σ is real, while σ' is pure imaginary when σ is complex. To determine n, we first recognize that from Eqs. (10) and (23), $y_2 = 0$ at $\theta = \theta_i$, while from Eq. (35b), $y_2 = \beta_i \sin \sigma$ at $\theta = \theta_f$ with $\beta_i > 0$. Hence a count is taken of the number of times $y_2(\theta)$ changes sign within the range of integration, $\theta_i \leq \theta \leq \theta_f$, but excluding the starting point.

If the result of this count is n', then we set $n = n'$ provided σ is real. In this case, since

$$\cos \sigma = (-1)^n \cos \sigma', \tag{36a}$$

from Eq. (36), and since $0 \leq \sigma' \leq \pi$, the value of σ' and hence σ is uniquely determined. Cyclops uses this method (instead of the one described above) to find ν_r or ν_z, and the resultant values should be correct in all cases (including the one cited above) provided only that the values are real.

However, if σ and hence ν_y are complex, we can have $n = n'$ or $n' + 1$, and to remove this ambiguity, we use the fact that $(-1)^n$ must match the sign of $\cos \sigma$ in this case. That is, since $\sigma = n\pi + i|\sigma'|$ here, then

$$\cos \sigma = (-1)^n \cosh|\sigma'|. \tag{36b}$$

When combined with the value found for n', this $\cos \sigma$ value determines both n and $|\sigma'|$, and hence the real and imaginary parts of $\nu_y = \sigma/\theta_0$. The program prints out the imaginary part in the column reserved for ν_r or ν_z, along with a special indicator as noted above. Directly after this number, it then prints (for brevity) the value of n, but this is sufficient to determine $\mathrm{Re}(\nu_y) = n\pi/\theta_0$, which must, of course, be a half integer. For simplicity, the integer n is always printed out following the value of ν_r or ν_z, which is somewhat redundant when the frequency is real.

Finally, we note that when σ is real, the values of α_i, β_i, and γ_i can be calculated from Eq. (35), and these quantities are needed later.

7. CALCULATION OF $\alpha(\theta)$ AND $\beta(\theta)$

As noted before, the program can be used to obtain much more detailed information about the linear oscillations than is contained in the values of ν_r and ν_z. That is, when σ is real and the motion is stable, and only in this case, the program will also provide values of $\alpha(\theta)$ and $\beta(\theta)$ as part of the long output.

If the phase-space vector (y, p_y) is represented by the column matrix $\mathbf{Q}$, then by extension of Eq. (12), we have

$$\mathbf{Q}(\theta) = \mathbf{Y}(\theta, \theta_i)\mathbf{Q}(\theta_i), \tag{37}$$

where $\mathbf{Y}(\theta, \theta_i)$ is the transfer matrix from θ_i to θ. Because of the periodicity of the magnet geometry, there is no physical distinction between the angles labeled θ and $\theta + \theta_0$. That is, for given y and p_y, the Hamiltonian is periodic in θ with period $\Delta\theta = \theta_0$.

As a consequence of this periodicity, we have the relation

$$\mathbf{Y}(\theta + \theta_0, \theta_i + \theta_0) = \mathbf{Y}(\theta, \theta_i), \tag{38a}$$

so that

$$\mathbf{Y}(\theta + \theta_0, \theta_i) = \mathbf{Y}(\theta, \theta_i)\mathbf{Y}(\theta_f, \theta_i), \tag{38b}$$

where here again $\theta_f = \theta_i + \theta_0$. This simply proves that a knowledge of $\mathbf{Y}(\theta, \theta_i)$ for one period, $\theta_i \leq \theta \leq \theta_f$, is sufficient to provide complete information about the general solution for all θ values.

The periodic transfer matrix $\mathbf{M}(\theta)$ can be defined as the operator that shifts $\mathbf{Q}(\theta)$ by one period, that is,

$$\mathbf{Q}(\theta + \theta_0) = \mathbf{M}(\theta)\mathbf{Q}(\theta), \tag{39}$$

and hence, from the previous equations, we have

$$\mathbf{M}(\theta) = \mathbf{Y}(\theta, \theta_i)\mathbf{Y}(\theta_f, \theta_i)\mathbf{Y}^{-1}(\theta, \theta_i). \tag{40}$$

It therefore follows that

$$\mathbf{M}(\theta_i) = \mathbf{Y}(\theta_f, \theta_i), \tag{41a}$$

and

$$\mathbf{M}(\theta + \theta_0) = \mathbf{M}(\theta), \tag{41b}$$

so that $\mathbf{M}(\theta)$ is periodic.

Equations (40) and (41) also show that $\mathbf{M}(\theta)$ is derived from $\mathbf{M}(\theta_i)$ by a similarity transformation, and it therefore follows that the determinant, the trace, and the eigenvalues of $\mathbf{M}(\theta)$ are all independent of θ. From the corresponding properties of $\mathbf{Y}(\theta_f, \theta_i)$ given in Eq. (33), we have

$$\|\mathbf{M}(\theta)\| = 1, \tag{42a}$$

$$M_{11}(\theta) + M_{22}(\theta) = 2\cos\sigma, \tag{42b}$$

and in addition, the eigenvalues of $\mathbf{M}(\theta)$ are

$$\lambda = \exp(\pm i\sigma). \tag{42c}$$

These properties allow us to represent $\mathbf{M}(\theta)$ in the standard form, as in Eq. (34), that is,

$$\mathbf{M}(\theta) = \mathbf{I}\cos\sigma + \mathbf{J}(\theta)\sin\sigma, \tag{43a}$$

where

$$\mathbf{J}(\theta) = \begin{pmatrix} \alpha(\theta) & \beta(\theta) \\ -\gamma(\theta) & -\alpha(\theta) \end{pmatrix} \tag{43b}$$

with

$$\beta(\theta)\gamma(\theta) - \alpha^2(\theta) = 1, \tag{43c}$$

so that $\gamma(\theta)$ can be determined from $\alpha(\theta)$ and $\beta(\theta)$. Since $\mathbf{M}(\theta)$ is periodic, so also are these functions. Moreover, for $\theta = \theta_i$, we have

$$\alpha(\theta_i) = \alpha_i, \qquad \beta(\theta_i) = \beta_i, \qquad \gamma(\theta_i) = \gamma_i, \tag{44}$$

where α_i, β_i, and γ_i are the same as those in Eq. (35).

In addition, Eqs. (40) and (43) lead to

$$\mathbf{J}(\theta) = \mathbf{Y}(\theta, \theta_i)\mathbf{J}(\theta_i)\mathbf{Y}^{-1}(\theta, \theta_i), \tag{45}$$

and after performing the multiplications, we finally obtain

$$\alpha(\theta) = \alpha_i(Y_{11}Y_{22} + Y_{12}Y_{21}) - \beta_i Y_{11}Y_{21} - \gamma_i Y_{12}Y_{22}, \tag{46a}$$

$$\beta(\theta) = \beta_i Y_{11}^2 + \gamma_i Y_{12}^2 - 2\alpha_i Y_{11}Y_{12}, \tag{46b}$$

where here, $Y_{jk} = Y_{jk}(\theta, \theta_i)$. These equations, together with the values of $Y_{jk}(\theta, \theta_i)$ obtained during the final integration, are the ones used by Cyclops to evaluate $\alpha(\theta)$ and $\beta(\theta)$. Actually, instead of $\beta(\theta)$, the program prints out the so-called width function, $w(\theta) = [\beta(\theta)]^{1/2}$, which is clarified in Section 9 below.

8. EIGENVECTORS

To understand the significance of $\alpha(\theta)$ and $\beta(\theta)$, we consider next the eigenvectors $\mathbf{Q}_+$ and $\mathbf{Q}_-$ of the operator $\mathbf{M}(\theta)$ corresponding to the eigenvalues $\lambda = \exp(\pm i\sigma)$, respectively. The matrix equation for $\mathbf{Q}_+$ is therefore

$$\mathbf{M}(\theta)\mathbf{Q}_+(\theta) = e^{i\sigma}\mathbf{Q}_+(\theta), \tag{47}$$

and since we are concerned only with real σ values, then $\mathbf{Q}_- = \mathbf{Q}_+^*$, the complex conjugate.

Repeated operation on the above equation with $\mathbf{M}(\theta)$ leads to the result

$$\mathbf{Q}_+(\theta + n\theta_0) = e^{in\sigma}\mathbf{Q}_+(\theta), \tag{48}$$

where n is an arbitrary integer; as a result, $\mathbf{Q}_+$ must have the Floquet form

$$\mathbf{Q}_+(\theta) = \mathbf{U}(\theta)\exp(i\nu_y\theta), \tag{49a}$$

with

$$\mathbf{U}(\theta)\begin{pmatrix} u(\theta) \\ v(\theta) \end{pmatrix}, \tag{49b}$$

where $u(\theta)$ and $v(\theta)$ are complex periodic functions having period θ_0.

Inserting this result together with $\mathbf{M}(\theta)$ from (43) into Eq. (47), and assuming $\sin\sigma \neq 0$, we finally obtain

$$v(\theta) = \frac{i - \alpha(\theta)}{\beta(\theta)}\, u(\theta), \tag{50}$$

which determines $v(\theta)$ from $u(\theta)$ when $\alpha(\theta)$ and $\beta(\theta)$ are given. This result, together with the Wronskian condition on $\mathbf{Q}_+$ and $\mathbf{Q}_-$ then yields

$$u^*(\theta)v(\theta) - u(\theta)v^*(\theta) = 2i\frac{|u(\theta)|^2}{\beta(\theta)} = 2iC_0, \tag{51}$$

where the normalization constant C_0 is positive and real.

For simplicity, C_0 should be chosen independent of the energy, and it proves most convenient to take $C_0 = 1$. For this choice, we then find

$$|u(\theta)|^2 = \beta(\theta), \qquad |v(\theta)|^2 = \gamma(\theta), \tag{52a}$$

and

$$u^*(\theta)v(\theta) = i - \alpha(\theta). \tag{52b}$$

Thus, $u(\theta)$ and $v(\theta)$ are completely determined except for a phase factor and to define this factor, we set

$$u(\theta) = [\beta(\theta)]^{1/2} \exp(i\delta(\theta)), \tag{53a}$$

so that

$$v(\theta) = [i - \alpha(\theta)][\beta(\theta)]^{-(1/2)} \exp(i\delta(\theta)), \tag{53b}$$

where $\delta(\theta)$ is as yet undetermined. Therefore, a complete description of the linear oscillations requires three real periodic functions, $\alpha(\theta)$, $\beta(\theta)$, and $\delta(\theta)$, together with the constant ν_y.

We should also note that the eigenvectors can be written in terms of the basic transfer matrix $\mathbf{Y}(\theta, \theta_i)$ as

$$\mathbf{Q}_+(\theta) = \mathbf{Y}(\theta, \theta_i)\mathbf{Q}_+(\theta_i), \tag{54}$$

which leads to expressions for $u(\theta)$ and $v(\theta)$ in terms of their values at θ_i. These expressions then yield the same equations for $\alpha(\theta)$ and $\beta(\theta)$ as those in Eqs. (46), but in addition, we find the equation for evaluating $\delta(\theta)$

$$\operatorname{cotan}(\nu_y(\theta - \theta_i) + \delta(\theta) - \delta_i) = \beta_i \frac{Y_{11}(\theta, \theta_i)}{Y_{12}(\theta, \theta_i)} - \alpha_i, \tag{55}$$

where $\delta_i = \delta(\theta_i)$ is arbitrary. Although Cyclops does not make use of this equation at present, it could readily be modified to do so if the need to calculate $\delta(\theta)$ should arise.

9. APPLICATIONS

Since the eigenvectors $\mathbf{Q}_+$ and $\mathbf{Q}_+^*$ are independent, they can also be used as a basis for representing the general solution; that is, we can write

$$\mathbf{Q}(\theta) = \frac{1}{2} A\mathbf{Q}_+(\theta) + \frac{1}{2} A^*\mathbf{Q}_+^*(\theta), \tag{56}$$

or, in terms of the components given in Eq. (49),

$$y(\theta) = \frac{1}{2} Au(\theta) \exp(i\nu_y\theta) + \text{c.c.}, \tag{56a}$$

$$p_y(\theta) = \frac{1}{2} Av(\theta) \exp(i\nu_y\theta) + \text{c.c.}, \tag{56b}$$

where A is some constant (complex) amplitude, and c.c. = complex conjugate. Moreover, A can be expressed in terms of the usual angle and action variables, ψ_0 and J, by setting

$$A = (2J)^{1/2} \exp(i\psi_0), \tag{57}$$

and if we then use Eqs. (53), we obtain

$$y(\theta) = [2J\beta(\theta)]^{1/2} \cos\psi, \tag{58a}$$

$$p_y(\theta) = -[2J/\beta(\theta)]^{1/2} (\sin\psi + \alpha(\theta)\cos\psi), \tag{58b}$$

where

$$\psi = \nu_y\theta + \delta(\theta) + \psi_0. \tag{58c}$$

Thus, the general solution can be written explicitly in terms of $\alpha(\theta)$, $\beta(\theta)$, $\nu_y\theta + \delta(\theta)$, and two real constants, ψ_0 and J.

If ψ is eliminated from the above expressions, we obtain the equation for the eigenellipse

$$\gamma(\theta)y^2 + \beta(\theta)p_y^2 + 2\alpha(\theta)yp_y = 2J, \tag{59}$$

with $\gamma(\theta)$ given by Eq. (43c). Thus, if we plot p_x vs x or p_z vs z once per sector for the orbit of any ion executing linear oscillations about the *EO*, we find that successive points fall on such an ellipse with an interval $\Delta\psi = \sigma = \nu_y\theta_0$. Evidently, the shape of the eigenellipse is determined by the periodic functions $\alpha(\theta)$ and $\beta(\theta)$.

The transformation $(y, p_y) \to (\psi_0, J)$ has a Jacobian determinant equal to unity, so that the area element is preserved, i.e., $dy\, dp_y = dJ\, d\psi_0$, as befits a canonical transformation. It follows in particular that the area of the above eigenelipse is $2\pi J$, so that its eccentricity and orientation may change with θ, but not its area (in agreement with Liouville's theorem).

As shown by Eq. (58a), the maximum value of $y(\theta)$ is

$$[y(\theta)]_{\max} = [2J\beta(\theta)]^{1/2}. \tag{60}$$

Consider now a beam of ions all at the same energy E, and suppose that their (y, p_y) phase-space points at the given θ completely fill the eigenellipse (59); that is, the jth particle has $J_j \leq J$, so that the emittance of this beam is $2\pi J/p$. It then follows that the radial or vertical width of this beam is given by

$$\Delta y = 2[2J\beta(\theta, E)]^{1/2}, \tag{61}$$

and since J is constant, this relation determines the width as a function of θ. As a result, we call $w(\theta, E) = [\beta(\theta, E)]^{1/2}$ the width function, while β itself is usually referred to as the amplitude function.[11] As an example, Fig. 3 shows plots of the radial and vertical width functions derived from the long output of Cyclops for the same cyclotron configuration as that used in obtaining Figs. 1 and 2.

Now it also happens that the action J is an adiabatic invariant, so that if the above beam is accelerated slowly, the relation (61) will specify the variation of the radial or vertical beam width as a function of E as well as θ. This important conclusion implies, for example, that a knowledge of $\beta(\theta, E)$ for the vertical oscillations allows one to

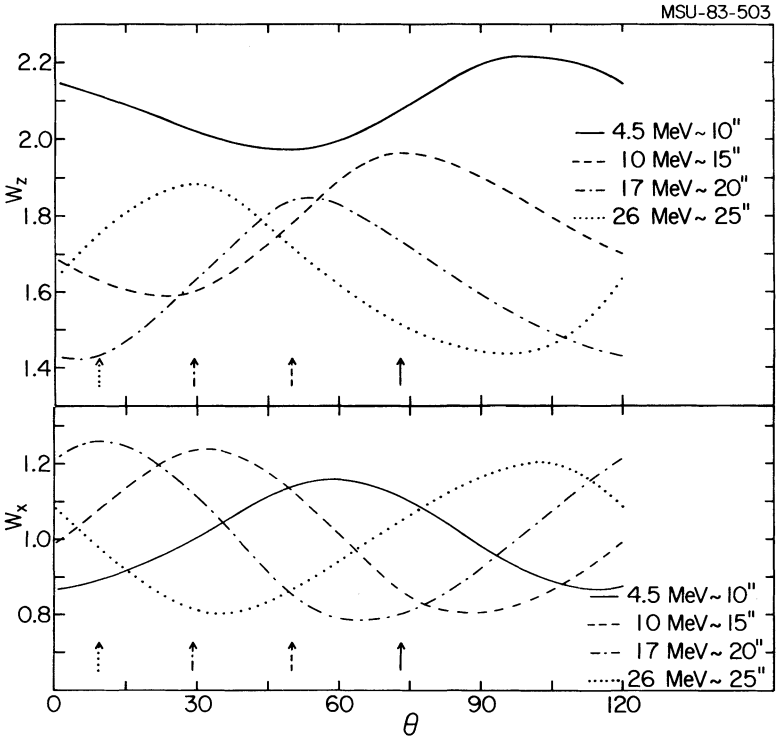

FIGURE 3 Graphs of radial and vertical width functions, W_x and W_z, as a function of θ for one sector, and for four different energies corresponding to $R \cong 10, 15, 20$, and 25 in. The vertical arrows mark the center of one hill which, evidently, shifts by 4.4 deg/in. because of the magnet spiral. The two edges of the hill are about $\pm 23°$ from the center, and as can be seen, the max (min) value of W_x or W_z occurs at the edge of the hill where the AG focusing has its max (min) strength. In our units, $p \cong R$, so that the average values of these functions defined in Eq. (65) are then given by $\bar{W}_y = (1/\nu_y)^{1/2}$, and the changes in these averages can therefore be understood from the behavior of ν_r and ν_z shown in Fig. 4.

predict the dependence of the beam height on r and θ, and hence the vertical acceptance of the cyclotron (but excluding the central region where the electric focusing and nonadiabatic effects cannot be neglected). This assumes that the size and shape of the beam emittance from the injector (or ion source plus central region) can be matched to the acceptance of the cyclotron, but even if this matching is not fully achieved in practice, the width function will still provide an upper bound for the beam envelope.

We should also note that the values of $\alpha(\theta)$ and $\beta(\theta)$ often prove useful in preparing certain input/output data for other programs which calculate accelerated orbits. For example, it is sometimes desirable to start a set of orbits with the same energy E and with (y, p_y) points on an eigenellipse of given area. This can be done quite systematically by calculating y and p_y from Eq. (58) above using ψ values which are uniformly spaced. That is, for the jth point, we take

$$\psi_j = \psi_m + j(2\pi/4n), \tag{62a}$$

where $j = 1, 2, \ldots, 4n$, with n being some integer, and where $\psi = \psi_m$ corresponds to the major or minor axis of the ellipse. Since the quantity $(y^2 + p_y^2)$ has its extrema at these points, we then find

$$\tan(2\psi_m) = \frac{2\alpha}{\beta^2 + \alpha^2 - 1}, \tag{62b}$$

where $0 \leq \psi_m < \pi/2$, to be specific. The resultant sequence of $4n$ points will subdivide each principal quadrant of the ellipse into n equal areas.

As another example, consider the set of accelerated orbits which are computed with the above initial conditions. If values of $\alpha(\theta, E)$ and $\beta(\theta, E)$ for one θ value and a broad range of E values are available, then the values of J and ψ for each accelerated orbit can be calculated once per sector as a function of energy using Eqs. (58). The results can then be examined to see whether, on the average, J = constant and $\Delta\psi = \sigma$, as would be expected if the motion is linear and adiabatic. On the other hand, if the computations correspond to the acceleration of this beam through some nonlinear resonance, for example, then the resultant increase in the J values will indicate the corresponding growth in the emittance area.

Finally, it should be noted that all the results in this and the preceding two sections have been derived without actually making use of the specific differential equations for y and p_y. If now the components of $\mathbf{Q}_+(\theta)$ given above are substituted into Eqs. (9) for the x-motion, or Eqs. (22) for the z-motion, one thereby obtains three first-order differential equations for the functions $\alpha(\theta)$, $\beta(\theta)$, and $\delta(\theta)$. Although we shall omit these equations here, certain conclusions are worth noting, especially since they differ somewhat from those customarily found in synchrotron work.[11]

First of all, we obtain the equation for ν_y:

$$\nu_y = \frac{1}{\theta_0} \int \frac{D(\theta)}{\beta(\theta)}\, d\theta, \tag{63}$$

where the integration runs from θ_i to $\theta_i + \theta_0$, and where $D(\theta)$ has one of the values

$$D(\theta) = rp^2/p_\theta{}^3, \qquad \text{for the } x\text{-motion}, \tag{64a}$$

or

$$D(\theta) = r/p_\theta, \qquad \text{for the } z\text{-motion.} \tag{64b}$$

The program should also provide for calculating ν_r and ν_z from this formula in order to confirm the results in those cases where the values look doubtful.

Equation (63) can also be used to define the average value of $\beta(\theta)$, thus

$$\bar{\beta} = \frac{R}{p\nu_y}, \tag{65}$$

where R is the average radius. The corresponding average width function is then $\bar{w} = (\bar{\beta})^{1/2}$, which is often used for approximate calculations.

As a further conclusion, we find that $\alpha(\theta)$ passes through zero at least twice in the period θ_0, and for the z-motion case, $\beta(\theta)$ has its maximum and minimum values at these points. On the other hand, when $\alpha = 0$ for the x-motion, the quantity β/r^2, rather than β itself, has an extremum.

10. PHASE-ENERGY RELATION

As noted in Section 5, the program calculates the orbit period τ as a function of the energy E, and hence the frequency error $\Omega(E)$ defined by

$$\Omega(E) = \nu_0\tau - 1 = \frac{\omega_0}{\omega} - 1, \tag{66}$$

where $\omega = 2\pi/\tau$, $\omega_0 = 2\pi\nu_0$, and ν_0 is part of the input. This $\Omega(E)$, which is part of the standard output at each E value, provides essential information for determining how well the given magnetic field conforms to the requirements of the rf system under consideration.

For cyclotrons, the phase ϕ of the ion relative to the rf is so defined that the average energy gain per turn is given by

$$\frac{dE}{dn} = qV\cos\phi, \tag{67a}$$

where V is the peak voltage gain per turn. For simplicity, we assume here that V is constant, and in this case, the average phase change per turn becomes

$$\frac{d\phi}{dn} = \omega_{rf}\tau - 2\pi h = 2\pi h\Omega(E), \tag{67b}$$

where $\omega_{rf} = h\omega_0$ is the rf angular frequency and h its harmonic number.

The first integral of these equations (or the Hamiltonian) then leads to the well known phase-energy relation

$$\sin\phi(E) = \sin\phi_i + \frac{2\pi h}{qV}\int \Omega(E)\,dE, \tag{68}$$

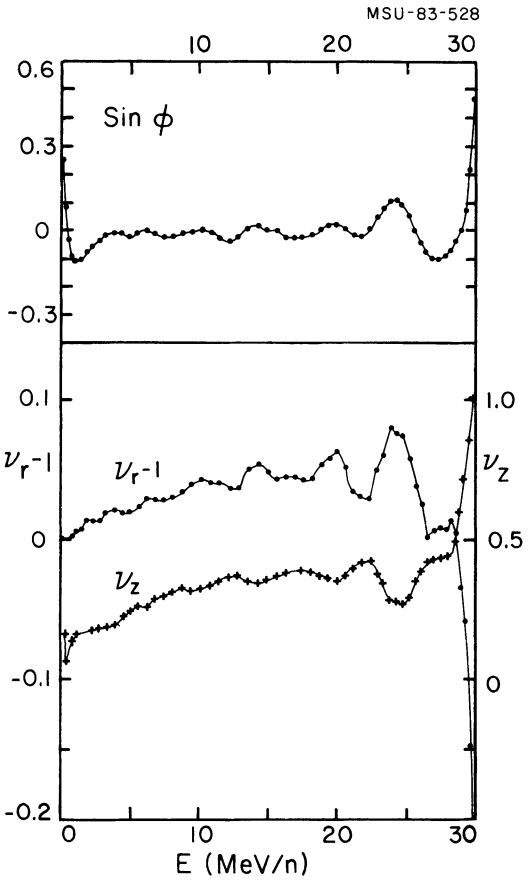

FIGURE 4 The upper graph shows sin ϕ vs E obtained for the same cyclotron field as that used for the other figures. In addition, it is assumed here that the initial phase $\phi_i = 30°$, the harmonic $h = 1$, and the peak energy gain per turn $qV = 60$ keV/A, which then leads to a total of about 500 turns. The lower two plots show the corresponding variations of $\nu_r - 1$ (left scale) and ν_z (right scale) with energy. The fine structure in these curves is produced by the discreteness of the 13 trim coils used to tailor the average field, and the correlation between the resultant oscillations in ν_r and ν_z should be noted. Moreover, these curves clearly show that from about 28 MeV/A to the extraction energy (30 MeV/A), the ions are accelerated out into the nonisochronous edge region of the field.

where the integral extends from the initial energy E_i where $\phi = \phi_i$ to the given energy E. An examination of the resultant ϕ vs E quickly shows whether the ion will reach the desired final energy in the given magnetic field.

Since the integral is the part of this relation that depends exclusively on the field properties, we separate out this factor by defining a phase-slip function F as

$$F(E) = 2\pi \int \Omega(E)\, dE, \tag{69}$$

and this quantity is furnished as part of the output along with $\Omega(E)$. If it is desired instead to have sin ϕ printed out, then the rf parameters V, h, and ϕ_i must be given as part of the input. Figure 4 shows a plot of sin ϕ vs E for the same cyclotron situation as that used for the other figures.

After the output has been inspected, it may seem desirable to modify the frequency ω_0 and it should be emphasized that such a change can be made quite easily without rerunning the program. That is, if a fractional shift ϵ' is made in the frequency, as defined by

$$\omega_0' = (1 + \epsilon')\omega_0, \tag{70}$$

then from the definition (66), the revised frequency error becomes

$$\Omega'(E) = (1 + \epsilon')\Omega(E) + \epsilon'. \tag{71}$$

As a result of Eq. (69), we then find that $F(E) \rightarrow F'(E)$ given by

$$F'(E) = (1 + \epsilon')F(E) + 2\pi\epsilon'(E - E_i). \tag{72}$$

Thus, since ϵ' is generally very small, this change produces a nearly linear shift of the sin ϕ vs E curve.

11. CONCLUDING REMARKS

Cyclotrons with radial sectors, like those at Indiana and GANIL in France, have extra magnetic symmetry and because of this, the *EO*'s in these machines have $p_r = 0$ at the center of each hill and valley. As a result, the calculation of normal *EO* and focusing properties requires orbit integration only through half a sector, i.e., from the center of a valley to the center of a hill (or vice versa). For such cases, we developed a special form of the *EO* Code which was then used in the final design of the Indiana cyclotron.[15]

It is also worth mentioning that an unusual overwrite has been incorporated into the TRIUMF version of Cyclops which enables the program to handle situations where the *EO* is slightly displaced from the nominal median plane as a result of magnet imperfections.[16] In addition to the usual map of B_z, this version of Cyclops requires values of B_r, B_θ, and $\partial B_z/\partial z$ in the place $z = 0$. It then uses modified equations of motion, which include zero- and first-order terms in z and p_z to calculate the displaced *EO* and the resultant focusing properties.

Since there exist now many individual *EO* Codes that have been developed at various laboratories, it seems highly desirable to have some standard cyclotron magnetic field established to serve as a test case for purposes of comparison. Such a field was devised by a group at SIN and this field has the twin virtues of being analytical in form and quite realistic as well. The relevant report[17] contains a listing for the subroutine that generates the field, together with a sample output.

In conclusion, I would like to express my gratitude to G. Mackenzie and his coworkers at TRIUMF for many useful discussions, and also to F. Marti and B. Milton for constructing the figures. Finally, I am most indebted to my wife Bernice, who continues to provide indispensible assistance as my reader and editor.

REFERENCES

1. M. M. Gordon and T. A. Welton, Oak Ridge National Lab., ORNL Report, 2765, (1959).
2. M. M. Gordon and W. S. Hudec, *Nucl. Instrum. Methods*, **18–19,** 243 (1962); M. M. Gordon and H. G. Blosser, *Ibid.*, 378.

3. L. Smith and A. A. Garren, Lawrence Berkeley Lab., UCRL Report 8598, January, 1959.
4. G. Parzen, *Ann. of Phys.*, **15,** 22 (1961).
5. H. L. Hagedoorn and N. F. Verster, *Nucl. Instrum. Methods*, **18–19,** 201 (1962).
6. M. M. Gordon, T. I. Arnette and D. A. Johnson, *Bull. APS*, **9,** 473 (1964).
7. W. Joho, Swiss Inst. for Nuclear Research, SIN Report TM-11-07, February, 1970.
8. G. Dutto, C. Kost, G. H. Mackenzie and M. K. Craddock, Cyclotrons-72, AIP Conf. Proc. 9 (Am. Inst. Phys., New York, 1972), p. 340; J. L. Bolduc and G. H. Mackenzie, *Ibid.*, p. 351.
9. C. J. Kost and G. H. Mackenzie, *IEEE Trans. Nucl. Sci.*, **NS–22,** 1922 (1975).
10. J. I. M. Botman, M. K. Craddock, C. J. Kost and J. R. Richardson, *IEEE Trans. Nucl. Sci.*, **NS–30,** 2007 (1983); R. Baartman, G. H. Mackenzie, R. Laxdal and R. Lee, *Ibid.*, 2010.
11. H. Bruck, "Circulation Particle Accelerators" Los Alamos Sci. Lab. Report LA-TR-72-10 Rev.; E. D. Courant, *Physics of High Energy Accelerators*, AIP Conf. Proc. 87 (Am. Inst. Phys., New York, 1982), p. 1.
12. M. M. Gordon, *Particle Accelerators*, **13,** 67 (1983).
13. M. M. Gordon, *Particle Accelerators*, **14,** 119 (1983).
14. H. Goldstein, *Classical Mechanics*, 2nd. ed. (Addison-Wesley, Reading, 1980), Section 11–7.
15. M. M. Gordon, *Ann. of Phys.*, **50,** 571 (1968); M. M. Gordon and D. A. Johnson, *Bull. APS*, **18,** 1422 (1973).
16. G. H. Mackenzie, TRIUMF Internal Report TRI-DN-72-10 (1972).
17. W. Joho, G. Rudolf and S. Adam, Swiss Inst. for Nuclear Research, SIN Report May 3, 1979.